Time Series Modeling of Alborzs Crustal Velocity by Using Artificial Neural Networks

Tohid Malekzade Dilmaghani
Department of Computer Engineering. Ahar Branch, Islamic Azad University, Ahar, Iran
tohidmelikzade@yahoo.com

Abstract

Artifitial neural network (ANN) is an information processing system that is formed by a large number of simple processing elements, known as artificial nerves. It is formed by a number of nodes and weights connecting the nodes. The input data are multiplied by the corresponding weights, and the summation are entered into neurons. The behavior of a neural network depends on the communication between nodes. Using the trained data, the designed ANN can be adjusted in an iterative procedure to determine optimal parameters of ANN. Then for an unknown input, we can compute corresponding output using the trained ANN.

There are many methods for training the network and modifications of the weights. One of the most famous and simplest methods is a back-propagation algorithm that trains the network in two stages: Feed-forward and feed-backward. In the feed-forward process, the input parameters are moved to the output layer. In this stage, the output parameters the next stage is done

In this study, a 3-layer perceptron neural network was used with 28 neurons in a hidden layer for modeling the eastern component (V_E) and 27 neurons in a hidden layer for modeling the northern component (V_N) velocity field of the earth's crust in Iran. Evaluation of the neural network model has been applied using 11 stations of GPS, and the velocity fields are defined with respect to the Eurasian plate. The minimum relative error obtained from this evaluation for the eastern component was -3.57% and for the northern component was +0.16%: also the maximum relative error for the eastern component was +38.1 % and for the northern component was +95.3%. In this study, a polynomial of degree 5 with 18 coefficients was used to model the east and north components for the evaluation of artificial neural networks in estimating the velocity rate of geodetic points. A comparison of the relative error from the polynomial model and the relative error from the neural network illustrated the superiority of the neural model with respect to the polynomial model in this region.

Keywords: Artificial neural network, crustal velocity, back-propagation algorithm, polynomial modeling

1. Introduction

Preliminary estimation of the Earth's crust velocity field, especially in seismic logic and near faults, can provide valuable information on the geodynamic structure as well as how faults operate. Networking is done by geodynamic stations. Figure 1 shows the shell velocity vectors in the Iranian region relative to the Eurasian plane. [1]

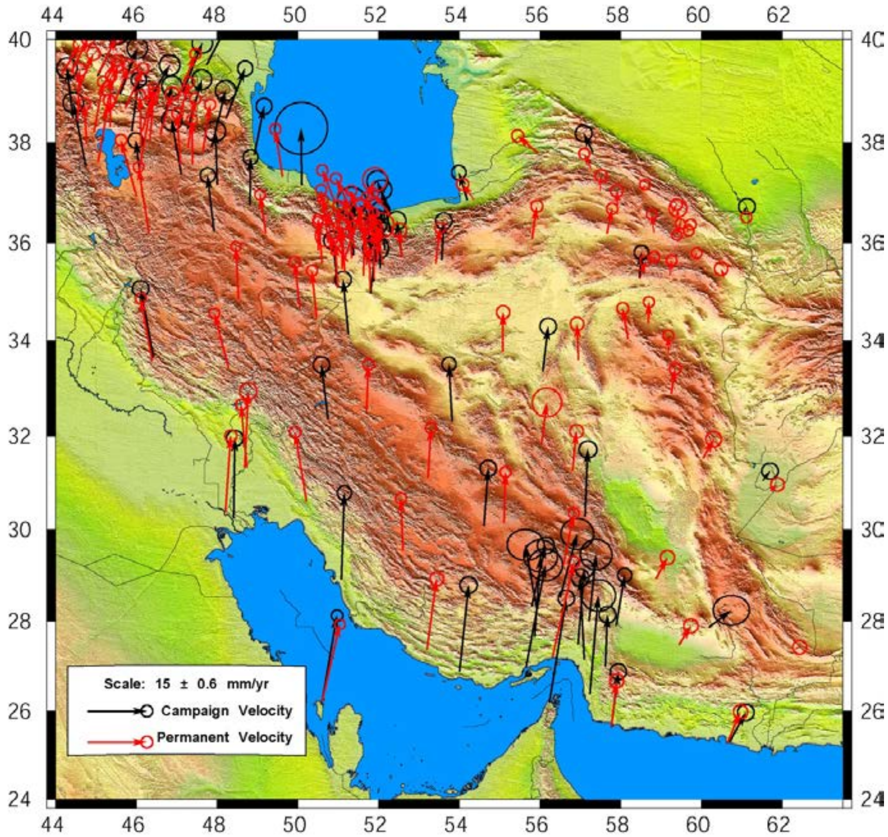

Figure 1: Crust velocity vectors in the region of Iran relative to the Eurasian plate taken from the site of the National Mapping Organization

The purpose of this paper is to compare the results of artificial neural networks in spatial estimation of velocity field in Iran. [2]

2. Theoretical Foundations

A neural network consists of the components of layers and weights. Network behavior also depends on communication between members [3]. In general, there are three types of neural layers in neural networks:

Input layer: Receive raw information that has been fed to the network.

Hidden layers: The performance of these layers is determined by the inputs and the weight of the connection between them and the hidden layers. The weights between the input and hidden units determine when a hidden unit should be activated. [4][5]

Output: The performance of the output unit depends on the activity of the hidden unit and the weight of the relationship between the hidden unit and the output.

In neural networks, there are several types of connections or weight links: Lead: Most links are of the type in which the signals move in only one direction. There is no feedback (loop) from input to output. The output of each layer does not affect the same layer. **[6]**

3. Materials and methods

In the error propagation algorithm, the excitation function of each nerve is considered as the sum of the weights of the inputs related to that nerve. Thus, assuming that w is the corresponding weights between the input layer and the next layer, we can write:

$$A_j(x,w)=\sum_{i=0}^{n} x_i w_{ji} \qquad (1)$$

It can be clearly seen that the nerve stimulation function depends only on the input and the corresponding weights[7][9]. Assuming that the output function is sigmoid, the output of the nth nerve can be written as follows:

$$O_j(x,w)=sgm\left(A_j(x,w)\right)=\frac{1}{1+e^{A_j(x,w)}} \qquad (2)$$

Carefully in Equation (3-4) we find that the output depends only on the value of the excitation function, which in turn is related to the input and the weights. Therefore, weights must be changed to change the output. [8]

$$E_j(x,w,d_j)=\left(O_j(x,w)-d_j\right)^2 \qquad (3)$$

The total network error can be written in the form of the sum of the errors of each of the nerves of the output layer. Therefore we have:

$$E(x,w,d)= \sum_j E_j(x,w,d_j)=\sum_j\left(O_j(x,w)-d_j\right)^2 \qquad (4)$$

Now we need to investigate the relationship between the error and the inputs, weights and outputs through the slope gradient method. [10]

In the slope gradient method, a quadratic cost function is first defined, which is:

$$J(w)= \frac{1}{N}\sum_{i=1}^{N} J(w,i)= \frac{1}{N}\sum_{i=1}^{N}\left(\frac{1}{2}\sum_{j=1}^{L_0}\left(O_j-d_j\right)^2\right) \qquad (5)$$

In relation (7-3) L0 is the output dimension (number of output layer neurons). The rate of change of weights at any time is:

$$\Delta w_{ji}=-\eta\frac{\partial E}{\partial w_{ji}} \qquad (6)$$

Where the weight correction constant is selected by the user. This constant determines the convergence rate of the algorithm [11] [12]. Using the chain rule we can write:

$$\frac{\partial E}{\partial w_{ji}}=\frac{\partial E}{\partial O_j}\times\frac{\partial O_j}{\partial w_{ji}} \qquad (7)$$

According to Equation (7-3) we can write

$$\frac{\partial E}{\partial O_j}=2\left(O_j-d_j\right) \qquad (8)$$

Also, by reusing the chain rule and considering relations (3-3) and (4-3), we can write:

$$\frac{\partial O_j}{\partial w_{ji}}= \frac{\partial O_j}{\partial A_j}\times\frac{\partial A_j}{\partial w_{ji}}=\left(O_j\left(1-O_j\right)\right)\times x_i \qquad (9)$$

In Equation (9-3) is used to calculate according to Equation (3-3) and with reference to the following property for the sigmoid function in which the derivative of the sigmoid function can be written according to the function itself: [13]

$$\frac{d}{dx}sgm(x)= \frac{d}{dx}\left(\frac{1}{1+e^{-x}}\right)=\frac{e^{-x}}{\left(1+e^{-x}\right)^2}= \left(1-smg(x)\right)sgm(x) \quad (10)$$

By placing (10-3) and (11-3) in the relation (9-3) we will have:

$$\frac{\partial E}{\partial w_{ji}}= \frac{\partial E}{\partial O_j}\times\frac{\partial O_j}{\partial w_{ji}}= 2\left(O_j-d_j\right)\times O_j\times\left(1-O_j\right)x_i \quad (11)$$

Now, by substituting (11-3) in (8-3) the final relation of the amount of weight correction in each step of the error propagation algorithm is obtained as follows:

$$\Delta w_{ji}= -\eta\frac{\partial E}{\partial w_{ji}}= -2\eta\left(O_j-d_j\right)\times O_j\times\left(1-O_j\right)x_i \quad (12)$$

4. Results

37main network stations were used to analyze the shell velocity field. The characteristics of statistical data used for the target network are given in Table -4)1.(

Table 1-4: Statistical specifications of input data

V_x (mm/yr)	**V_y (mm/yr)**	**V_z (mm/yr)**	
-0/071	-0/0589	-0/06	**max**
0/1984	0/4172	0/248	**min**
-0/0196	0/0152	0/0198	**Average**
0/0389	0/0696	0/0421	**Standard deviation**

Figure (4-1) shows the spatial distribution of these 37 stations. In this figure, the black triangle represents the stations used as the input of all three methods and the red circles represent the test stations. Out of 37 stations, 4 stations have been selected as test stations. [15][16] The spatial distribution of these 4 stations is such that it can provide a correct assessment of the accuracy of the results obtained from all three methods.

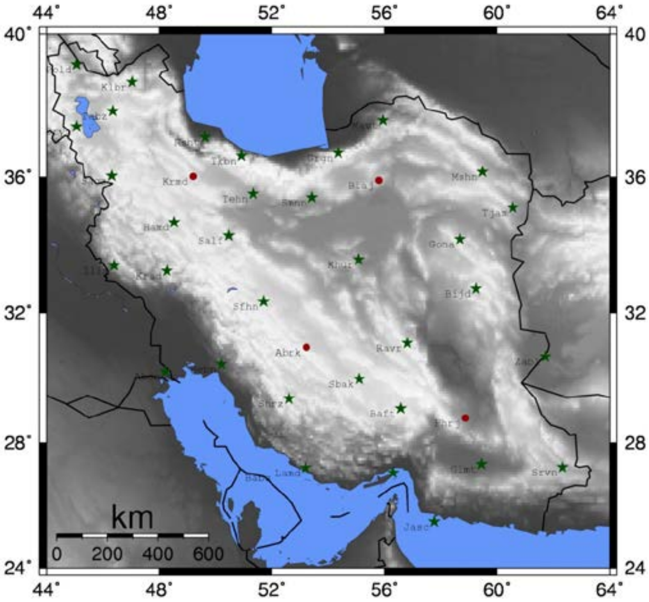

Figure 4-1: How to spatially distribute the stations used

Processing observations Shows the velocity vectors in the region of Iran relative to the Eurasian plate with a 95% error ellipse (velocity vectors obtained by Berness v.4.2 software).

The stations used in this research are divided into three groups: 30 stations to train the network after error propagation, 3 stations to evaluate the network error and 4 stations to test the results obtained from the modeled artificial neural network.

Figure (2-4) shows the velocity field met at other geodetic points on the Iranian plateau by means of an artificial neural network.

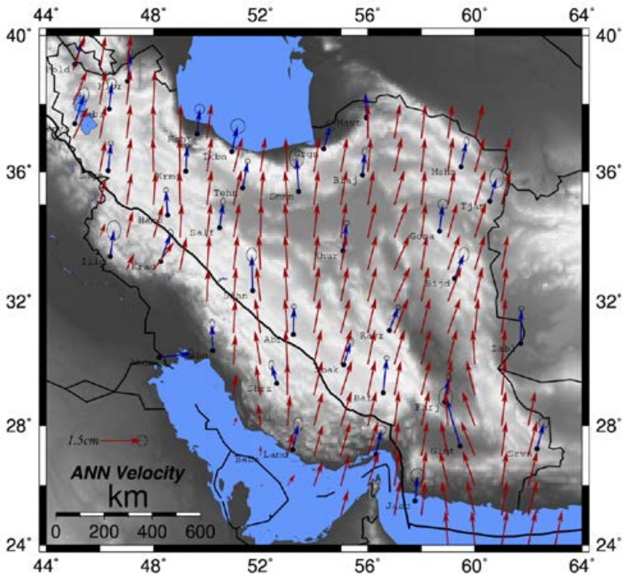

Fig 2-4: Estimated velocity vectors using a three-layer neural network relative to the Eurasian plane

Tables (1-4) and (2-4) show the relative speed and error values obtained from GPS and ANN models for the eastern and northern components at 4 test stations.

Table 2-4: Speed and relative error values obtained from GPS, ANN models for Eastern component (VE) at 4 test stations

Statation name	**Latitude (deg)**	**Longitude (deg)**	**GPS Velocity (m/yr)**	**ANN. Velocity (m/yr)**	**Relative Error (%) (GPS- ANN)**
Krmd	36.012	49.210	-0.0318	-0.027	10.83
Biaj	35.903	55.805	-0.02553	-0.027	14.70
Abrk	30.950	53.226	-0.02941	-0.025	8.73
Fhrj	28.774	58.881	-0.0427	-0.029	17.74

Table 3-4: Speed and relative error values obtained from GPS, ANN models for the northern component (VN) at 4 test stations

Statation name	**Latitude (deg)**	**Longitude (deg)**	**GPS Velocity (m/yr)**	**ANN. Velocity (m/yr)**	**Relative Error (%) (GPS- ANN)**
Krmd	36.012	49.210	-0.00198	0.002	17.00
Biaj	35.903	55.805	0.00967	0.016	1.51
Abrk	30.950	53.226	0.00057	0.003	4.16
Fhrj	28.774	58.881	-0.00897	0.013	17.75

According to the above figures and tables, it can be concluded that the results obtained from artificial neural networks in estimating the speed of geodetic points, both in direction and in a small amount, have a significant agreement with the results obtained from GPS processing [17]. Table (4-4) shows the velocity field values obtained from GPS processing, the velocity values estimated by the artificial neural network, and the relative error values at the 4 test stations.

Table 4-4: Value field values obtained from processing and estimated speed field from artificial neural network with relative errors in selected test stations in the target network

station	**Speed field obtained from GPS (m / yr)**			**Estimated velocity field (m / yr)**			**Relative error (%)**		
	V_E	**V_N**	**V_z**	**V_E**	**V_N**	**V_z**			
Krmd	-0.0318	-0.00198	0.00961	-0.027	0.002	0.00842	10.83	17.00	12.38
Biaj	-0.02553	0.00967	0.01612	-0.027	0.016	0.0201	14.70	1.51	24.69
Abrk	-0.02941	0.00057	0.01618	-0.025	0.003	0.01842	8.73	4.16	13.84
Fhrj	-0.0427	-0.00897	-0.00366	-0.029	0.013	-0.00402	17.74	17.75	9.84

Neural network efficiency analysis in Central Alborz network

Tables (5-4) and (6-4) show the relative speed and error values obtained from GPS and ANN models for the eastern and northern components at two test stations.

Table 5-4: Speed and relative error values obtained from GPS, ANN models for Eastern component (VE) at 2 test stations

Statation name	**Latitude (deg)**	**Longitude (deg)**	**GPS Velocity (m/yr)**	**ANN. Velocity (m/yr)**	**Relative Error (%) (GPS- ANN)**
Amad	35.521	52.586	0.00411	0.00367	10.71
Akht	35.406	50.6	0.00337	0.00249	26.11

Table 6-4: Speed and relative error values obtained from GPS, ANN models for the northern component (VN) at 2 test stations

Statation name	**Latitude (deg)**	**Longitude (deg)**	**GPS Velocity (m/yr)**	**ANN. Velocity (m/yr)**	**Relative Error (%) (GPS- ANN)**
Amad	35.521	52.586	0.00411	0.02564	1.46
Akht	35.406	50.6	0.00337	0.0364	9.45

According to the results obtained in Tables (7-4) and (8-4), it can be concluded that the minimum relative error obtained from the artificial neural network is 10.71% for the northern component and 1.46% for the component. East and the maximum relative error value is 26.11% for the northern component and 9.45% for the eastern component of the velocity field. Table (4-10) shows the velocity field values obtained from GPS processing, the velocity values estimated by the artificial neural network, and the relative error values at the two test stations. [18]

Table 7-4: Values of speed fields obtained from processing and estimated speed field from artificial neural network with relative errors in selected test stations in the desired network

station	**Speed field obtained from GPS (m / yr)**			**Estimated velocity field (m / yr)**			**Relative Error (%)**		
	V_E	**V_N**	**V_Z**	**V_E**	**V_N**	**V_Z**			
Amad	0.00411	0.00411	0.01309	0.00367	0.02564	0.01421	10.71	1.46	8.56
Akht	0.00337	0.00337	0.01678	0.00249	0.0364	0.0111	26.11	9.45	33.85

5. Discussion and conclusion

In the neural network model, a 3-layer structure with 25 neurons in the hidden layer was used to estimate the velocity field of the geodetic points. The number of hidden layer neurons was determined based on trial and error and based on the minimum relative error generated at the test points. With this structure, the average relative error generated at the test points was + 13.48 for the northern component and + 18.12 for the eastern component of the velocity field. The results indicate the relative superiority of the artificial neural network model in estimating the velocity field in the region of Iran. As a suggestion for future research, it is possible to use a suitable station distribution with a large number to evaluate the efficiency of this method, especially near active faults.

Refrence:

[1] Djamour Y. & Vernant Ph. & Bayer R. & Nankali H. R. & Ritz J. F. Hinderer J. & Hatam Y. & Luck B. & Moigne N. L. & Sedighi M. & Khorrami F. 2010 - GPS and gravity constraints on continental deformation in the Alborz mountain range, Iran, Geophys. J. Int., 183, 3, 1287-1301.

[2] Aoki Y, Scholz C (2003) Vertical Deformatin Of The Japanese Islands, 1996-1999. J Geophysics Res 108, 2257 No. B5, 2257, doi:10.1029/2002JB002129, 2003

[3] Bogusz, J, Klos, A, GRZEMPOWSKI, P, KONTNY, B, (2013) “Modelling the Velocity Field in a Regular Grid in the Area of Poland on the Basis of the Velocities of European Permanent Stations”, Pure and Applied Geophysics, DOI 10.1007/s00024-013-0645-2.

[4] Guest B. & Axen G. J. & Lam P. S. & Hassanzadeh J. - 2006a, Late Cenozoic shortening in the west-central Alborz Mountains, northern Iran, by combined conjugate strike-slip and thinskinned deformation, Geosphere, 2, 35-52.

[5] Masson F., Chéry J., Hatzfeld D., Martinod J., Vernant P., Tavakoli F., Ghafory-Ashtiani M (2007): " Large-scale velocity field and strain tensor in Iran inferred from GPS measurements: new insight for the present-day deformation pattern within NE Iran." Journal of Geophysics: 170:436-440.

[6] BEALE, M.H. , HAGAN, M.T. , DEMUTH, H.B. (2010) “Neural Network Toolbox 7 User’s Guide”. The MathWorks Inc., Natick, MA, 951 pp.,

[7] Chan WS, Xu YL, Ding XL, Dai WJ (2006) An integrated GPS-accelerometer data processing technique for structural deformation monitoring J Geod 80:705-719

[8] Coukuyt, I, Dhaene, T, Demeester, P, (2013), “ooDace toolbox: a matlab Kriging toolbox, getting started”,

[9] Engdahl E. R. & Jackson J. A. & Myers S. C. & Bergman E. A. & Priestley, K., 2006 – Relocation and assessment of seismicity in the Iran region, Geophys. J. Int., 167, 2, 761-778.

[10] Neves M. C. & Paiva L. T. & Luis J. 2009 - Software for slip-tendency analysis in 3D: A plug-in for Coulomb, Computers and Geosciences, 35, 12, 2345-2352.

[11] Rueger J. M., (2006), Overview of geodetic deformation measurements of dams, NCOLD conference on dams and annual general meeting, November 2006, Australia.

[12] VanGorp, S, Masson, F, Chéry, J, (2006) “The use of Kriging to interpolate GPS velocity field and its application to the Arabia-Eurasia collision zone”, Geophysical Research Abstracts, Vol. 8, 02120

[13] Grafarend E. W, Moghtasad Azar Kh,(2007) Surface deformation analysis of GPS dense Network based on intrinsic geometry deterministic and stochastic aspects J Geod.

[14] Heidbach O. & Tingay M. & Barth A. & Reinecker J. & Kurfeß D. & Müller B. (eds.) 2008 – The World Stress Map, Commission for the Geological Map of the World, Paris, 1:46M.

[15] Hossainali, M. M. (2006). "A Comprehensive Approach to the Analysis of the 3Dkinematics of Deformation." PhD Thesis, Geodesy. Darmstadt, University of Darmstadt.

[16] MOGHTASED-AZAR, K. ZALETNYIK, P. (2009) “Crustal velocity field modeling with neural network and polynomials”, In: SIDERIS, M.G. (Ed.), Observing our changing Earth, International Association of Geodesy Symposia, 133, pp. 809-816,

[17] MUSTAFA YILMAZ, (2013) “ARTIFICIAL NEURAL NETWORKS PRUNING APPROACH FOR GEODETIC VELOCITY FIELD DETERMINATION”, BCG - Boletim de Ciências Geodésicas,

[18] M.R. Ghaffari, B.Vosooghi, (2014) “2Dimentinal Crustal Deformation Analysis Using IPGN Data”, International Geosciences Congress.